

Preparative and Structural Studies on the Carbonyl Cyanides of Iron, Manganese, and Ruthenium: Fundamentals Relevant to the Hydrogenases

Stephen M. Contakes, Sodio C. N. Hsu, Thomas B. Rauchfuss,* and Scott R. Wilson

Department of Chemistry, University of Illinois at Urbana-Champaign, Urbana, Illinois 61801

Received October 4, 2001

The reaction of cyanide, carbon monoxide, and ferrous derivatives led to the isolation of three products, *trans*- and *cis*-[Fe(CN)₄(CO)₂]²⁻ and [Fe(CN)₅(CO)]³⁻, the first two of which were characterized by single-crystal X-ray diffraction. The new compounds show self-consistent IR, ¹³C NMR, and mass spectroscopic properties. The reaction of *trans*-[Fe(CN)₄(CO)₂]²⁻ with Et₄NCN gives [Fe(CN)₅(CO)]³⁻ via a first-order (dissociative) pathway. The corresponding cyanation of *cis*-[Fe(CN)₄(CO)₂]²⁻, which is a minor product of the Fe(II)/CN⁻/CO reaction, does not proceed at measurable rates. Methylation of [Fe(CN)₅(CO)]³⁻ gave exclusively *cis*-[Fe(CN)₄(CNMe)(CO)]²⁻, demonstrating the enhanced nucleophilicity of CN⁻ *trans* to CN⁻ vs CN⁻ *trans* to CO. Methylation has an electronic effect similar to that of protonation as determined electrochemically. We also characterized [M(CN)₃(CO)]ⁿ⁻ for Ru (*n* = 1) and Mn (*n* = 2) derivatives. The Ru complex, which is new, was prepared by cyanation of a [RuCl₂(CO)₃]₂ solution.

Introduction

While cyanide is often discussed in terms of its π -acceptor properties, the most dominant characteristic of this ligand is its potency as a σ -donor.¹ Because of its strong donor properties, cyanide stabilizes the binding of carbon monoxide to metals in intermediate oxidation states. In contrast, stoichiometrically related M–CO–halide derivatives tend to be less stable. The ability of cyanide to promote the complexation of π -acceptor ligands is probably related to the catalytic properties of the cobaltcyanides.²

The ability of cyanometalates to stabilize CO binding and to promote transformations of small molecules has come into focus because of the presence of cyanide at the active sites of the two major families of hydrogenases, the Fe-only and the Fe–Ni hydrogenases.^{3–9} The biosynthesis of such bio-

organometallic centers is a fascinating and incompletely resolved issue, although recently Bock et al. have isolated a possible precursor to the CN⁻ and CO ligands.¹⁰ Our interests in this theme stem from a desire to prepare active site analogues of the hydrogenases from preassembled Fe–CN–CO building blocks. For example, the Ni–Fe hydrogenases feature [Fe(CO)(CN)₂]{Ni(μ -SR)₂(SR)₂} sites that could in principle be assembled by the reaction of Fe(CO)(CN)₂-containing precursors with a preformed nickel tetrathiolate. There are, however, no suitable sources of an Fe(CO)(CN)₂ fragment (e.g., Fe(CN)₂(CO)₄). Prior to our efforts¹¹ and those of Koch,¹² the only known Fe–CN–CO compounds were [Fe(CN)(CO)₄]⁻,¹³ [Fe₂(μ -CN)(CO)₈]⁻,¹⁴ and [Fe(CN)₅(CO)]³⁻.¹⁵ Liaw has shown that [Fe(CN)(CO)₄]⁻ is a useful precursor to Fe–CN–CO–SR species.¹⁶

Because of the undeveloped state of Fe–CN–CO chemistry, we undertook the present exploratory project aimed at expanding the range of Fe(II)–CN–CO derivatives. This

* Author to whom correspondence should be addressed. E-mail: rauchfuz@uiuc.edu.

- (1) Dunbar, K. R.; Heintz, R. A. *Prog. Inorg. Chem.* **1997**, *45*, 283–391.
- (2) Halpern, J.; Guastalia, G.; Bercaw, J. *Coord. Chem. Rev.* **1972**, *8*, 167–173 and references therein.
- (3) Volbeda, A.; Garcin, E.; Piras, C.; de Lacey, A. L.; Fernandez, V. M.; Hatchikian, E. C.; Frey, M.; Fontecilla-Camps, J. C. *J. Am. Chem. Soc.* **1996**, *118*, 12989.
- (4) Peters, J. W.; Lanzilotta, W. N.; Lemon, B. J.; Seefeldt, L. C. *Science* **1998**, *282*, 1853–1858.
- (5) Peters, J. W. *Curr. Opin. Struct. Biol.* **1999**, *9*, 670–676.
- (6) Pierik, A. J.; Roseboom, W.; Happe, R. P.; Bagley, K. A.; Albracht, S. P. J. *J. Biol. Chem.* **1999**, *274*, 3331–3337.
- (7) Nicolet, Y.; Piras, C.; Legrand, P.; Hatchikian, C. E.; Fontecilla-Camps, J. C. *Structure* **1999**, *7*, 13–23.

- (8) Adams, M. W. W.; Stiefel, E. I. *Curr. Opin. Chem. Biol.* **2000**, *4*, 214–220.
- (9) Nicolet, Y.; de Lacey, A. L.; Vernede, X.; Fernandez, V. M.; Hatchikian, E. C.; Fontecilla-Camps, J. C. *J. Am. Chem. Soc.* **2001**, *123*, 1596–1601.
- (10) Paschos, A.; Glass, R. S.; Bock, A. *FEBS Lett.* **2001**, *488*, 9–12.
- (11) Rauchfuss, T. B.; Contakes, S. M.; Hsu, S. C. N.; Reynolds, M. A.; Wilson, S. R. *J. Am. Chem. Soc.* **2001**, *123*, 6933–6934.
- (12) Jiang, J.; Koch, S. A. *Angew. Chem., Int. Ed.* **2001**, *40*, 2629–2631.
- (13) Goldfield, S. A.; Raymond, K. N. *Inorg. Chem.* **1974**, *13*, 770–775.
- (14) Ruff, J. K. *Inorg. Chem.* **1969**, *8*, 86–89.
- (15) Muller, J. A. C. R. *Hebd. Seances Acad. Sci.* **1887**, *104*, 992.

Table 1. Known M–CO–CN Derivatives^a

| group VIA M = Cr, Mo, W | group VIIA M = Mn, Re | group VIIIA | | |
|--|---|---|--|--|
| [M(CN)(CO) ₅] ⁻ | M(CN)(CO) ₅ | [Fe(CN)(CO) ₄] ⁻ | [Co(CN)(CO) ₃] ²⁻ | [Ni(CN) ₂ (CO) ₂] ²⁻ |
| [M(CN) ₂ (CO) ₄] ²⁻ | [M(CN) ₂ (CO) ₄] ⁻ | [Fe ₂ (CN)(CO) ₈] ⁻ | [Co ₂ (CN) ₂ (CO) ₆] ²⁻ | [Ni(CN)(CO) ₃] ⁻ |
| [M(CN) ₃ (CO) ₃] ³⁻ | [M(CN) ₃ (CO) ₃] ²⁻ | [Fe(CN) ₃ (CO) ₃] ⁻ | [Co(CN) ₃ (CO) ₂] ²⁻ | |
| [M(CN) ₄ (CO) ₂] ⁴⁻ | [M(CN) ₄ (CO) ₂] ³⁻ | [Fe(CN) ₄ (CO) ₂] ²⁻ | [Rh(CN) ₂ (CO) ₂] ⁻ | |
| [Cr ₂ (CN)(CO) ₁₀] ⁻ | Re ₃ (CN) ₃ (CO) ₁₂ | [Fe(CN) ₅ (CO)] ³⁻ | [Rh(CN) ₃ (CO)] ²⁻ | |
| | | [Ru(CN) ₃ (CO) ₃] ⁻ | | |
| | | [Ru ₆ (CN) ₂ (CO) ₂₀] ²⁻ | | |

^a Entries are from ref 21 except [Fe(CN)₃(CO)₃]⁻,²⁰ [Fe(CN)₄(CO)₂]²⁻,^{11,12,20} [Ru(CN)₃(CO)₃]⁻ (this work), [Ni(CN)(CO)₃]⁻,²² [Ru₆(CN)₂(CO)₂₀]²⁻,²³ and Re₃(CN)₃(CO)₁₂.²⁴

has resulted in the synthesis of *trans*-[Fe(CN)₄(CO)₂]²⁻ and *cis*-[Fe(CN)₄(CO)₂]²⁻ and a new route to [Fe(CN)₅(CO)]³⁻.^{17–19} In complementary work, we describe [Ru(CN)₃(CO)₃]⁻ and [Mn(CN)₃(CO)₃]²⁻; Jiang and Koch have recently described [Fe(CN)₃(CO)₃]⁻.²⁰ A list of known M–CO–CN derivatives is presented in Table 1.^{21–24}

Results

Synthesis of *trans*- and *cis*-[Fe(CN)₄(CO)₂]²⁻ and [Fe(CN)₅(CO)]³⁻. Treatment of MeCN suspensions of FeCl₂ with CO followed by the addition of 4 equiv of Et₄NCN afforded yellow solutions containing three anions, *trans*-[Fe(CN)₄(CO)₂]²⁻ (**1**), *cis*-[Fe(CN)₄(CO)₂]²⁻ (**2**), and [Fe(CN)₅(CO)]³⁻ (**3**), Figure 1 and Scheme 1. Addition of PPh₄⁺ precipitated both **1** and **2**, which were further purified by extraction into MeCN. The dominant product was the *trans* isomer. The trianion **3** does not form a water-insoluble PPh₄⁺ salt. Instead, **3** was precipitated using the more hydrophobic PPN⁺ (PPN⁺ = bis(triphenylphosphine)iminium cation) after removing the two dicarbonyl derivatives. We also examined the reaction of FeCl₂ with CO followed by the addition of 3 equiv of Et₄NCN in MeCN, which afforded a yellow suspension. The IR spectroscopy of the MeCN solution also indicated the formation of complexes **1**, **2**, and **3** in low yield. IR spectra for the crude reaction mixtures showed no evidence for tricarbonyl species.

The three products were identified by IR and ¹³C NMR spectroscopy; additionally each compound gave well-resolved ESI-mass spectra with molecular ions. The IR spectrum of *trans*-[Fe(CN)₄(CO)₂]²⁻ (**1**) exhibits one ν_{CO} band at 1999 cm⁻¹ whereas the *cis* isomer **2** had two ν_{CO} bands at 2042 and 1994 cm⁻¹. The ν_{CN} bands at 2103, 2119, and 2108 cm⁻¹ were also diagnostic for the *trans* and *cis* isomers, respectively. The structure of the isomers was further confirmed by ¹³C NMR measurements in the CO/CN region, which showed the correct multiplicity.

Characterization of pentacyanide **3** was also straightforward, except that its properties are somewhat dependent on

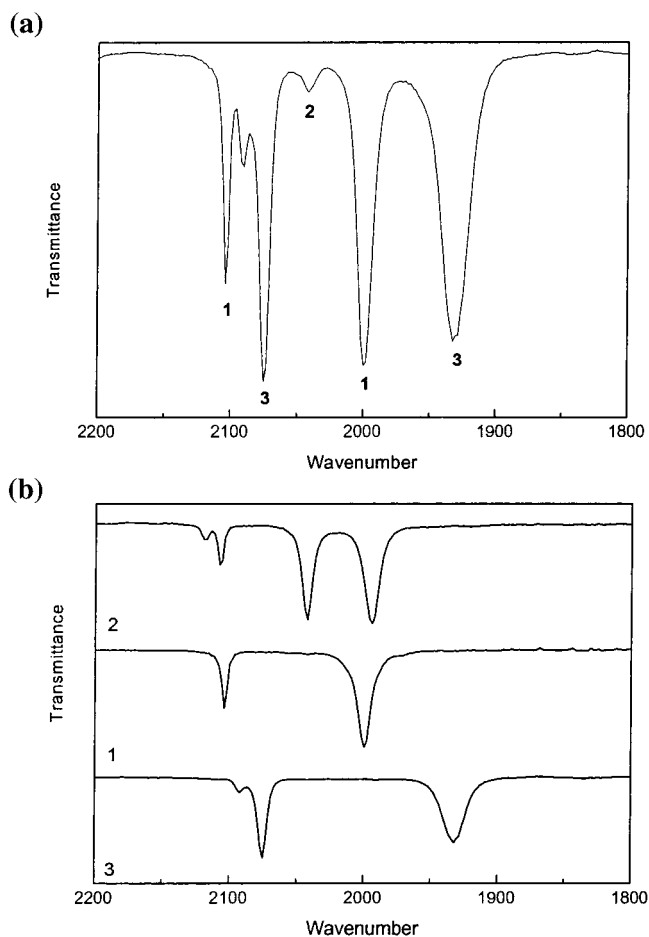


Figure 1. (a) IR spectrum of FeCl₂ + CO + CN⁻ mixture in MeCN solution. (b) IR spectra of MeCN solutions of *cis*-[Fe(CN)₄(CO)₂]²⁻ (**2**), *trans*-[Fe(CN)₄(CO)₂]²⁻ (**1**), and [Fe(CN)₅(CO)]³⁻ (**3**).

its solvation. Other cyanometalates are known to be solvatochromic (*vide infra*), but this behavior had not been observed with the carbonyl cyanide series. Freshly isolated (PPN)₃[Fe(CN)₅(CO)] is white, but upon drying in *vacuo* it becomes deep yellow. The IR spectrum of the yellow form of (PPN)₃[Fe(CN)₅(CO)] exhibits ν_{CN} at 2090 and 2075 cm⁻¹ and one ν_{CO} at 1932 cm⁻¹. The corresponding white (PPN)₃-[Fe(CN)₅(CO)] showed ν_{CN} bands at 2094 (shoulder) and 2077 cm⁻¹ and one ν_{CO} band at 1946 cm⁻¹ in MeCN solution. Addition of 1 equiv of H₂O to a MeCN solution of (PPN)₃[Fe(CN)₅(CO)] shifted the ν_{CO} band to higher energy,

(16) Liaw, W.-F.; Lee, N.-H.; Chen, C.-H.; Lee, C.-M.; Lee, G.-H.; Peng, S.-M. *J. Am. Chem. Soc.* **2000**, *122*, 488–494.

(17) Soria, D. B.; Aymonino, P. J. *Spectrochim. Acta* **1999**, *55A*, 1243–1253.

(18) Toma, H. E.; Moroi, N. M.; Iha, N. Y. M. *An. Acad. Bras. Cienc.* **1982**, *54*, 315–323.

(19) Toma, H. E.; Creutz, C. *Inorg. Chem.* **1977**, *16*, 545–550.

(20) Jiang, J.; Koch, S. A. *Inorg. Chem.* **2002**, *41*, 158–160.

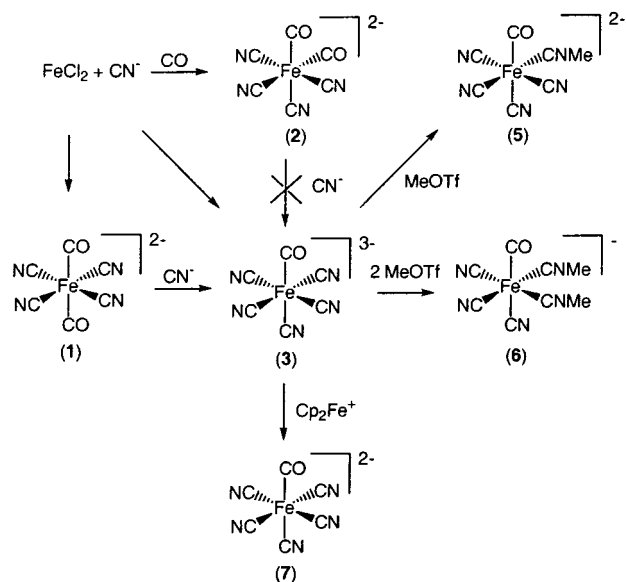
(21) Sharpe, A. G. *The Chemistry of Cyano Complexes of the Transition Metals*; Academic Press: London, 1976.

(22) Joo, F.; Alper, H. *Organometallics* **1985**, *4*, 1775–1778.

(23) Lavigne, G.; Luga, N.; Bonnet, J. J. *J. Chem. Soc., Chem. Commun.* **1987**, 957–958.

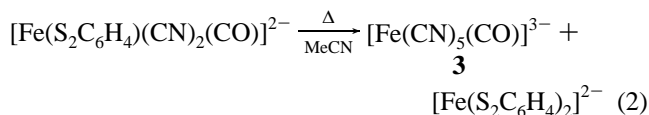
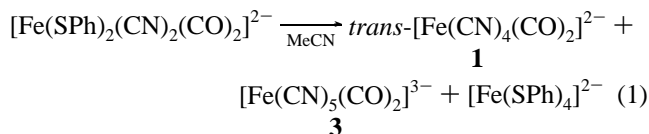
(24) Calderazzo, F.; Mazzi, U.; Pampaloni, G.; Poli, R.; Tisato, F.; Zanazzi, P. F. *Gazz. Chim. Ital.* **1989**, *119*, 241–247.

Scheme 1



from 1932 to 1968 cm^{-1} . Collectively, our data are consistent with the colorless form of **3** being subject to hydrogen bonding. The dicarbonyls **1** and **2** are not visibly solvatochromic, probably because their absorption maxima are shifted more deeply into the UV.

We previously studied the compounds $[\text{Fe}(\text{CO})_2(\text{CN})_2(\text{SPh})_2]^{2-}$ and $[\text{Fe}(\text{S}_2\text{C}_6\text{H}_4)(\text{CO})(\text{CN})_2]^{2-}$.¹¹ We found that in solution both species decompose to give a mixture of *trans*-**1** and **3** species, as determined by IR measurements. We demonstrated that a coproduct of this decomposition is $[\text{Fe}(\text{SR})_4]^{2-}$ demonstrated by crystallographic characterization of $(\text{Et}_4\text{N})_2[\text{Fe}(\text{SR})_4]$.



Product Distribution and Mechanistic Considerations.

The distribution of **1**–**3** from the carbonylation of ferrous cyanide solutions was relatively unaffected when 5 equiv of Et_4NCN was used in place of 4 equiv. When the synthesis was conducted using aqueous KCN, however, the pentacyanide **3** became the dominant product. High temperatures also favor **3** (see Table 2). We propose that some **3** arises via decarbonylation of *trans*- $[\text{Fe}(\text{CN})_4(\text{CO})_2]^{2-}$ under these conditions. Indeed upon heating, a solution of *trans*-(PPh_4)₂- $[\text{Fe}(\text{CN})_4(\text{CO})_2]^{2-}$ gave a 42% isolated yield of the pentacyanide **3**. On the other hand, the thermolysis also produced 3% *cis*-isomer **2** and a yellow insoluble product **4**, which is proposed to be a polymer. The yellow polymer **4** reacts with CN^- to give **3**.

We examined the preparation of iron cyanides where $\text{CN}^-/\text{Fe} < 6$ in the absence of CO with the goal of identifying

Table 2. Yield Data for Reactions Leading to Fe–CN–CO Derivatives

| reactants | T ($^\circ\text{C}$), time | solvent | products (% yield) | | |
|--|-----------------------------------|----------------------|--------------------|----------|----------|
| | | | 1 | 2 | 3 |
| FeCl_2 , Et_4NCN (4 equiv), 1 atm of CO | 25 | MeCN | 39% | trace | 36% |
| FeCl_2 , Et_4NCN (5 equiv), 1 atm of CO | 25 | MeCN | 38% | trace | 42% |
| FeCl_2 , Et_4NCN (4 equiv), ^a 1 atm of CO | 82 | MeCN | not detected | 9% | 54% |
| FeCl_2 , Et_4NCN (5 equiv), ^a 1 atm of CO | 82 | MeCN | not detected | 4% | 80% |
| FeCl_2 , KCN (4 equiv), 1 atm of CO | 25 | H_2O | 9% | trace | 32% |

^a The reaction also produced a yellow insoluble product **4**.

Table 3. Rate Constants for the Reaction of 0.0156 M **1** and 0.156 M Et_4NCN in MeCN and EtCN (369 K)^a

| temp (K) | $(10^6)k$, s^{-1} |
|----------|-----------------------------|
| 324 | 6.5 |
| 336 | 66.6 |
| 355 | 628.9 |
| 369 | 2033.6 |

^a The fit indicates $\Delta H^\ddagger = 29.3$ (2.8) kcal/mol and $\Delta S^\ddagger = 9.0$ (7.8) cal/(K mol) (numbers in parentheses indicate standard deviation).

possible reaction intermediates. The reaction of 4 equiv of Et_4NCN with a MeCN suspension of FeCl_2 gave a deep red-orange solution. If after 1 h this solution is treated with CO, the dominant product is **3**. On the other hand, treatment of this red solution with 9,10-phenanthroline gave $[\text{Fe}(\text{CN})_4(\text{phen})]^{2-}$, isolated as its bis(PPN^+) salt. This blue salt is highly solvatochromic, giving red solutions in water. Solvatochromism is a well-known characteristic for iron cyanides.^{25–28} The K^+ salt of this anion has been reported previously.²⁹

We examined the kinetics of the reaction of Et_4NCN with *trans*- $[\text{Fe}(\text{CN})_4(\text{CO})_2]^{2-}$ (**1**) to give $[\text{Fe}(\text{CN})_5(\text{CO})]^{3-}$ (**3**) at various concentrations of excess cyanide and at various temperatures. The rate of reaction is unaffected by $[\text{CN}^-]$ over the concentration range 0.1–0.5 M. This observation is consistent with a dissociative mechanism, which is expected for the substitution at an octahedral $18 e^-$ complex. The temperature dependence of the rate of the reaction was examined at four temperatures over the range 51–96 $^\circ\text{C}$ (Table 3). The analysis of these results using the usual Eyring approach gave ΔH^\ddagger of 29.3 ± 2.8 kcal/mol and ΔS^\ddagger of 9.0 ± 7.8 cal/K·mol. Representative IR spectra for the reaction of **1** with 10 equiv of CN^- to give **3** is shown in Figure 2. We also examined the reaction of the *cis* isomer **2** with excess Et_4NCN in refluxing MeCN solution. No reaction was detected by IR spectroscopy, i.e., the *cis* isomer is less labile than the *trans* isomer.

Structure of *trans*- and *cis*- $[\text{Fe}(\text{CN})_4(\text{CO})_2]^{2-}$. The structures of *cis*- and *trans*- $[\text{Fe}(\text{CN})_4(\text{CO})_2]^{2-}$ are presented in Figures 3 and 4, respectively. Both are octahedral

(25) Garcia, P.; Marques, J.; Pereira, E.; Gameiro, P.; de Castro, B.; Salema, R. *Chem. Commun.* **2001**, 1298–1299.

(26) Gameiro, P.; Maia, A.; Pereira, E.; de Castro, B.; Burgess, J. *Transition Met. Chem.* **2000**, *25*, 283–286.

(27) Tlaczala, T.; Bartecki, A. *Monatsh. Chem.* **1997**, *128*, 225–234.

(28) Burgess, J.; Lane, R. C.; Singh, K.; Castro, B. d.; Santos, A. P. G. d. *J. Chem. Soc., Faraday Trans.* **1994**, *90*, 3071–3075.

(29) Schilt, A. A. *J. Am. Chem. Soc.* **1960**, *82*, 3000–3005.

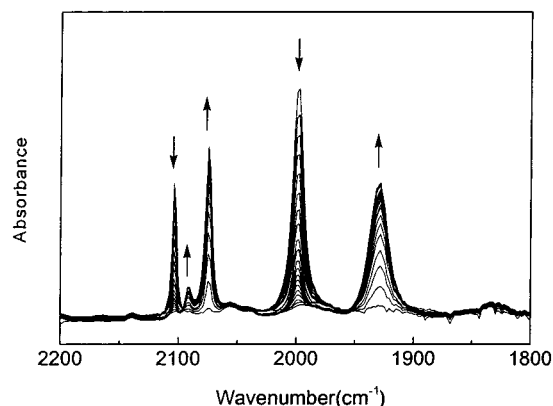


Figure 2. IR spectra for formation of $[\text{Fe}(\text{CN})_5(\text{CO})]^{3-}$ (**3**) from 0.0156 M *trans*- $[\text{Fe}(\text{CN})_4(\text{CO})_2]^{2-}$ (**1**) and 10 equiv of Et_4NCN at 82 °C in MeCN solution. The spectra were recorded at intervals of 5 min and, after 70 min, at intervals of 10 min. Duration of the experiment is 120 min.

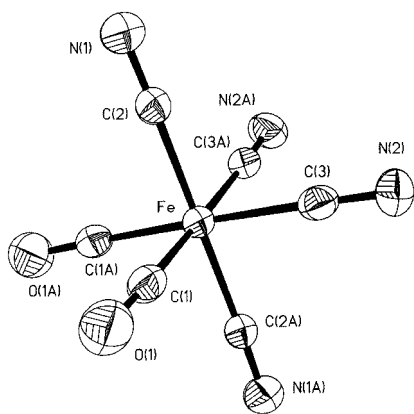


Figure 3. Molecular structure of the anion *cis*- $[\text{Fe}(\text{CN})_4(\text{CO})_2]^{2-}$ with thermal ellipsoids drawn at the 50% level.

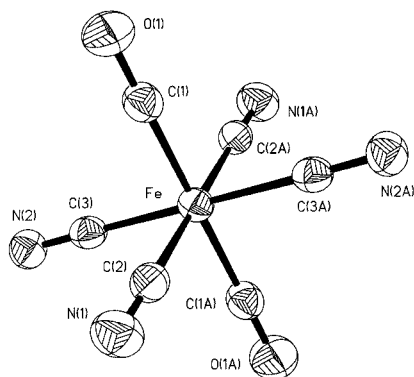


Figure 4. Molecular structure of the anion *trans*- $[\text{Fe}(\text{CN})_4(\text{CO})_2]^{2-}$ with thermal ellipsoids drawn at the 50% level.

complexes. The *cis* isomer **2** has two crystallographically imposed symmetry planes, one containing C1–O1, C1A–O1A, C3–N3, C3A–N3A; the other plane bisects the angle C1–Fe–C1A and C3–Fe–C3A and contains C2–N1, Fe, C2A–N1A. The *trans* isomer **1** is centrosymmetric crystallographically.

The Fe–CO distances of 1.81 Å for *trans* isomer **1** and 1.85 Å for *cis* isomer **2** are considerably shorter than those observed for the isoelectronic homoleptic carbonyl complex $[\text{Fe}(\text{CO})_6]^{2+}$ (1.911 Å)³⁰ and are indicative of extensive back-

Table 4. Selected Bond Distances (Å) for *trans*- $[\text{Fe}(\text{CN})_4(\text{CO})_2]^{2-}$ (**1**), *cis*- $[\text{Fe}(\text{CN})_4(\text{CO})_2]^{2-}$ (**2**), and *cis*- $[\text{Fe}(\text{CN})_4(\text{CNMe})(\text{CO})]^{2-}$ (**5**)

| parameter | 1 | 2 | 3 |
|-----------|----------|----------|----------|
| Fe–CO | 1.811(3) | 1.847(2) | 1.781(6) |
| Fe–CN | 1.937(3) | 1.940(3) | 1.920(5) |
| | 1.940(3) | 1.954(3) | 1.933(6) |
| Fe–CNMe | | | 1.942(6) |
| C–O | 1.133(3) | 1.157(3) | 1.165(5) |
| C–N | 1.143(3) | 1.159(3) | 1.160(4) |
| | 1.145(3) | 1.166(3) | 1.161(6) |
| C–NMe | | | 1.171(6) |
| CN–Me | | | 1.161(6) |
| | | | 1.430(0) |

bonding. In contrast, the Fe–CN distances of 1.93–1.96 Å (Table 4) are consistent with the predominantly σ character of the Fe–CN bond.

Alkylation of $[\text{Fe}(\text{CN})_5(\text{CO})]^{3-}$. We examined the methylation of **3** using MeOTf in order to understand the charge distribution in this complex. The *cis* cyanide ligands in $[\text{Fe}(\text{CN})_5\text{NO}]^{2-}$ exhibit enhanced nucleophilicity toward metal electrophiles.^{31–34} The reaction of **3** with 1 equiv of MeOTf produced *cis*- $[\text{Fe}(\text{CN})_4(\text{CNMe})(\text{CO})]^{2-}$ (**5**) as the exclusive product. Analytically pure samples of this yellow salt were obtained by mechanical separation of the yellow crystals from the PPNOTf coproduct. One CNMe singlet was observed in the ¹H NMR spectrum, and the ¹³C NMR spectrum showed four signals in the CN region consistent with the low symmetry of this complex compared with **3** (see above). Spectroscopic studies show that dimethylation of **3** gave *fac*- $[\text{Fe}(\text{CN})_3(\text{CNMe})_2(\text{CO})]^{-}$ (**6**). The stereochemistry of this salt was established by the observation of two ν_{CNMe} bands at 2223 and 2198 cm^{-1} and two ν_{CN} bands at 2113 and 2103 cm^{-1} , in addition to the ν_{CO} band at 2009 cm^{-1} . The ¹H NMR spectrum of $[\text{Fe}(\text{CN})_3(\text{CNMe})_2(\text{CO})]^{-}$ also shows only one Me signal consistent with the facial structure.

The structure of $[\text{Fe}(\text{CN})_4(\text{CNMe})(\text{CO})]^{2-}$ (**5**) was confirmed by single-crystal X-ray diffraction (Figure 5). The anion is octahedral with the CNMe ligand *cis* to CO. A crystallographic (mirror) plane contains C1, C2, C4, and C5. The Fe–CO distance of 1.78 Å in **5** is shorter by 0.07 Å than that in *cis*- $[\text{Fe}(\text{CN})_4(\text{CO})_2]^{2-}$ (Table 4), consistent with the strong σ -donor role of the CNMe vs CO ligand. Two research groups^{35,36} have recently reported the crystallographic characterization of $[\text{Fe}(\text{CN})_5(\text{CO})]^{3-}$; they found Fe–CO distances of 1.75–9 Å, consistent with our results. In contrast, the Fe–CNMe distance of 1.86 Å also is shorter

(30) Bernhardt, E.; Bley, B.; Wartchow, R.; Willner, H.; Bill, E.; Kuhn, P.; Sham, I. H. T.; Bodenbinder, M.; Broechler, R.; Aubke, F. *J. Am. Chem. Soc.* **1999**, *121*, 7188–7200.

(31) Clemente-Leon, M.; Coronado, E.; Galan-Mascaros, J. R.; Gomez-Garcia, C. J.; Woike, T.; Clemente-Juan, J. M. *Inorg. Chem.* **2001**, *40*, 87–94.

(32) Gu, Z.-Z.; Sato, O.; Einaga, Y.; Kai, M.; Iyoda, T.; Fujishima, A.; Hashimoto, K. *Bull. Chem. Soc. Jpn.* **2001**, *74*, 1617–1622.

(33) Forlano, P.; Parise, A. R.; Olabe, J. A. *Inorg. Chem.* **1998**, *37*, 6406–6407.

(34) Corbella, M.; Monfort, M.; Ribas, J. Z. *Anorg. Allg. Chem.* **1986**, *543*, 233–240.

(35) Jiang, J.; Acunzo, A.; Koch, S. A. *J. Am. Chem. Soc.* **2001**, *123*, 12109–12110.

(36) Baraldo, L. M.; Forlano, P.; Parise, A. R.; Slep, L. D.; Olabe, J. A. *Coord. Chem. Rev.* **2001**, *219–221*, 881–921.

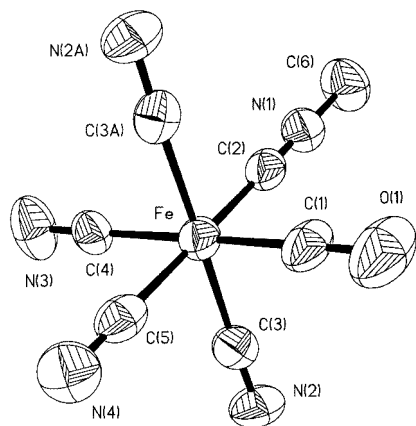


Figure 5. Molecular structure of the anion $cis\text{-}[\text{Fe}(\text{CN})_4(\text{CNMe})(\text{CO})]^{2-}$ with thermal ellipsoids drawn at the 50% level.

Table 5. Redox Couples for $[\text{Fe}(\text{CN})_{6-x}(\text{CO})_x]^{n-}$ Complexes

| compound | $E_{1/2}$ (mV) vs NHE |
|--|-----------------------|
| $[\text{Fe}(\text{CN})_6]^{4- a}$ | -609 |
| $[\text{Fe}(\text{CN})_5(\text{CO})]^{3- b}$ (3) | -443 |
| $trans\text{-}[\text{Fe}(\text{CN})_4(\text{CO})_2]^{2- b}$ (1) | 1417 |
| $cis\text{-}[\text{Fe}(\text{CN})_4(\text{CO})_2]^{2- b}$ (2) | 1607 |

^a Conditions: scan rate 50 mV/s; 1 mM in MeCN.⁴³ ^b Conditions: scan rate 200 mV/s; 1 mM in MeCN.

than Fe–CN distances of 1.92–1.94 Å, indicative of the predominantly σ -donor character of the cyanide ligand. The expected order of π -acceptor strength is $\text{CN}^- < \text{CNMe} < \text{CO}$. Complex **5** is a rare example of a complex containing CO, CNMe, and CN ligands.

Qualitatively, protonation of **3** supports the findings from the methylation. Addition of 1 equiv of HOTf to a solution of **3** shifts the ν_{CO} band to 1973 cm^{-1} , a shift of $\sim 50 \text{ cm}^{-1}$. A similar difference in ν_{CO} exists between **3** and **5**. Addition of a further 1 equiv of HOTf to **3** gave white precipitates, which are likely to be hydrogen-bond-bridged polymers similar to $\text{H}_4\text{Fe}(\text{CN})_6$.³⁷

Redox Properties of $[\text{Fe}(\text{CN})_5(\text{CO})]^{3-}$. Given the low value of ν_{CO} for this trianion **3**, we expected that it should be possible to generate the corresponding ferric carbonyl. Few ferric carbonyl complexes are known.^{38–42} The cyclic voltammetry of a MeCN solution of **3** confirmed the ease of oxidation, with a reversible couple occurring at $E_{1/2} \sim 443 \text{ mV}$ vs NHE. This value is ca. 1100 mV more positive than that for $[\text{Fe}(\text{CN})_6]^{4-}$ under the same conditions (the redox potential of $[\text{Fe}(\text{CN})_6]^{4-}$ is highly sensitive to medium effects⁴³). By comparison the *cis* and *trans* dicarbonyls **1** and **2** oxidize at $> 1 \text{ V}$ (Table 5). We also found that the addition

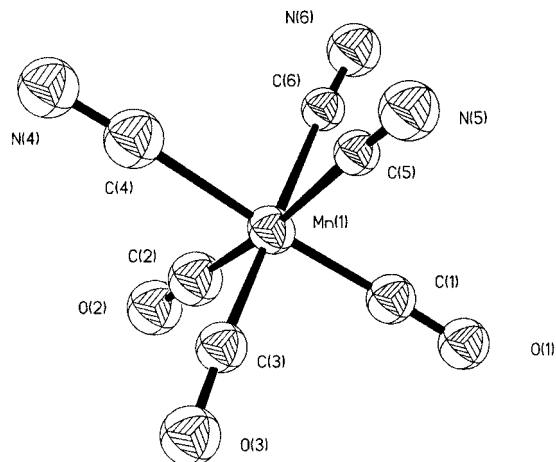


Figure 6. Molecular structure of the anion $fac\text{-}[\text{Mn}(\text{CN})_3(\text{CO})_3]^{2-}$ with thermal ellipsoids drawn at the 50% level.

Table 6. Selected Bond Distances (Å) and Angles (deg) for Two Molecules in the Asymmetric Unit of the Anion in $(\text{PPh}_4)_2[\text{fac}\text{-}[\text{Mn}(\text{CN})_3(\text{CO})_3]^{2-}]$

| parameter | molecule 1 | molecule 2 |
|--------------|------------|------------|
| Mn–CO | 1.751(17) | 1.758(17) |
| | 1.784(16) | 1.804(18) |
| | 1.792(19) | 1.835(19) |
| Mn–CN | 1.993(17) | 1.970(16) |
| | 2.013(16) | 1.984(18) |
| | 2.019(15) | 2.055(17) |
| C–O(av) | 1.172 | 1.145 |
| C–N(av) | 1.156 | 1.145 |
| OC–Mn–CO(av) | 92.3 | 93.1 |
| NC–Mn–CN(av) | 88.1 | 87.3 |

of small amounts of water or phenol lowered the oxidation potential of **3**. For example, the addition of 1 equiv of H_2O to a MeCN solution of **3** resulted in a shift in $E_{1/2}$ from 443 to 629 mV; these results are consistent with the effect of water on the IR spectrum and the color of **3** (see above).

Encouraged by the CV results, we generated $[\text{Fe}(\text{CN})_5(\text{CO})]^{2-}$ (**7**) using ferrocenium as the oxidant. This reaction afforded a red-brown solution. The IR spectrum of **7** exhibits ν_{CN} bands at 2127 and 2096 cm^{-1} . The ν_{CO} band at 1980 cm^{-1} is shifted by 48 cm^{-1} to higher energy relative to $[\text{Fe}(\text{CN})_5(\text{CO})]^{3-}$ (**3**) (see above). Under N_2 , $(\text{PPN})_2[\text{Fe}(\text{CN})_5(\text{CO})]$ (**PPN-7**) was stable in MeCN solution for hours at room temperature.

Synthesis and Structure of $[\text{M}(\text{CN})_3(\text{CO})_3]^{n-}$ Salts ($\text{M} = \text{Mn}, n = 2; \text{M} = \text{Ru}, n = 1$). The Ru and Mn derivatives were examined as analogues of $[\text{Fe}(\text{CN})_3(\text{CO})_3]^-$. The synthesis of the Mn derivative was previously described by Behrens,⁴⁴ but we streamlined the procedure: Addition of PPh_4Cl to an aqueous extract of the high-temperature reaction residue of $\text{Mn}(\text{CO})_5\text{Cl}$ and KCN gave a 55% yield of $(\text{PPh}_4)_2[\text{Mn}(\text{CN})_3(\text{CO})_3]$. Crystallographic analysis of this salt revealed two similar molecules of $fac\text{-}[\text{Mn}(\text{CN})_3(\text{CO})_3]^{2-}$ in the asymmetric unit, one of which is shown in Figure 6. The Mn–CO vs M–CN linkages of both molecules were assigned on the basis of Mn–C distances, because the former are typically 0.1–0.2 Å shorter (Table 6). The IR spectrum

(37) Ginsberg, A. P.; Koubek, E. *Inorg. Chem.* **1965**, *4*, 1186–1194.

(38) Hsu, H.-F.; Koch, S. A.; Popescu, C. V.; Münck, E. *J. Am. Chem. Soc.* **1997**, *119*, 8371–8372.

(39) Vergamini, P. J.; Kubas, G. J. *Prog. Inorg. Chem.* **1976**, *21*, 261–282.

(40) Delville-Desbois, M.-H.; Mross, S.; Astruc, D.; Linares, J.; Varret, F.; Rabaã, H.; Le Beuze, A.; Saillard, J.-Y.; Culp, R. D.; Atwood, D. A.; Cowley, A. H. *J. Am. Chem. Soc.* **1996**, *118*, 4133–4147.

(41) Morrow, J.; Catheline, D.; Desbois, M. H.; Manriquez, J. M.; Ruiz, J.; Astruc, D. *Organometallics* **1987**, *6*, 2605–2607.

(42) Etzenhouser, B. A.; Cavanaugh, M. D.; Spurgeon, H. N.; Sponsler, M. B. *J. Am. Chem. Soc.* **1994**, *116*, 2221–2222.

(43) Mascharak, P. K. *Inorg. Chem.* **1986**, *25*, 245–247.

(44) Behrens, H.; Ruyter, E.; Lindner, E. *Z. Anorg. Allg. Chem.* **1967**, *349*, 251–257.

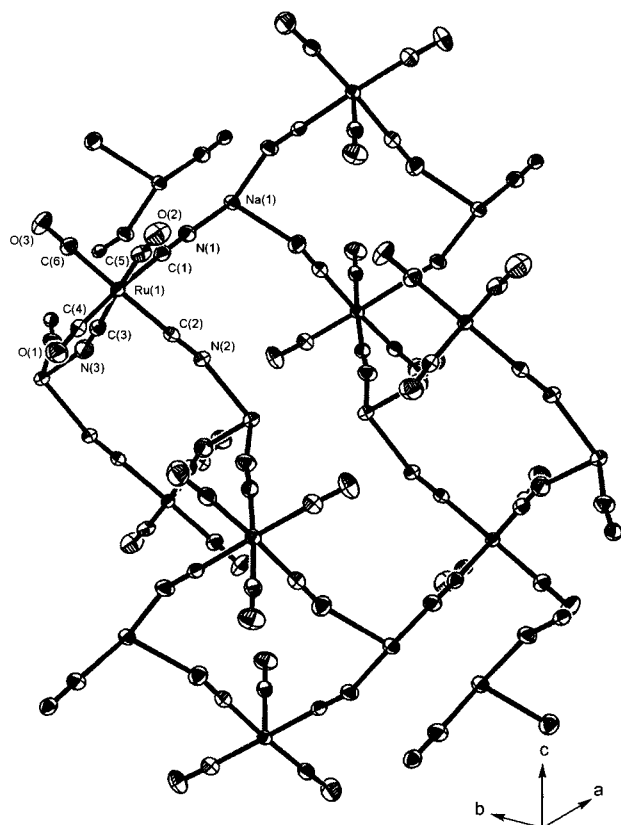
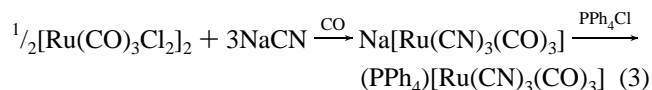


Figure 7. Structural diagram of the three-dimensional lattice showing the interaction of Na cations with the $[\text{Ru}(\text{CN})_3(\text{CO})_3]^-$ anions; the DMF is omitted for clarity.

of $\text{fac}-(\text{PPh}_4)_2[\text{Mn}(\text{CN})_3(\text{CO})_3]$ exhibits pairs of ν_{CN} and ν_{CO} bands at 2110 and 2097 cm^{-1} and 1993 and 1904 cm^{-1} , respectively.

The Ru(II) analogue of the Mn(I) compound, $[\text{Ru}(\text{CN})_3(\text{CO})_3]^-$, is a new anion. This colorless species was prepared by the addition of cyanide to a carbonylated solution of ruthenium trichloride under CO followed by precipitation using PPh_4^+ (eq 3). The IR spectrum of $\text{PPh}_4[\text{Ru}(\text{CN})_3(\text{CO})_3]$



exhibits ν_{CN} bands at 2163 and 2144 cm^{-1} and ν_{CO} bands at 2117 and 2075 cm^{-1} , consistent with the facial isomer. ^{13}C NMR measurements revealed one CO singlet at $\delta 188$ and one CN singlet at $\delta 122.99$. Only one cyano carbonyl of Ru is known, a derivative of $\text{Ru}_3(\text{CO})_{12}$.²³ Crystallographic analysis of $\text{Na}(\text{DMF})[\text{Ru}(\text{CN})_3(\text{CO})_3]$ confirmed the expected structure for the anionic metal center. The anion is linked to a polymeric framework wherein all CN ligands are coordinated via N– Na^+ linkages (Figure 7). Each Na^+ center is additionally coordinated to two DMF ligands, which also bridge to another Na^+ atom. The Ru–CO distances are shorter than Ru–CN distances by $\sim 0.1 \text{ \AA}$ (Table 7), as also observed for Fe–CO–CN complexes discussed above. The NC–Ru–CN bond angles are 87.8°, the slight deviation from 90° being attributable to complexation to the Na–DMF network.

Table 7. Selected Bond Distances (Å) and Angles (deg) for $\text{fac-Na}(\text{DMF})[\text{Ru}(\text{CN})_3(\text{CO})_3]$

| | | | |
|--------|----------|--------------|-----------|
| Ru1–C1 | 2.078(4) | C–O(av) | 1.12 |
| Ru1–C2 | 2.064(4) | C–N(av) | 1.15 |
| Ru1–C3 | 2.056(4) | OC–Ru–CO(av) | 93.7 |
| Ru1–C4 | 1.948(4) | NC–Ru–CN(av) | 87.8 |
| Ru1–C5 | 1.952(4) | Ru–C–O(av) | 175.6 |
| Ru1–C6 | 1.970(4) | Ru–C–N(av) | 176.6 |
| N1–Na1 | 2.495(4) | C1–N1–Na1 | 166.3(3) |
| Na1–O4 | 2.324(3) | N1–Na1–O4 | 84.08(12) |
| O4–C7 | 1.243(4) | Na1–O4–C7 | 143.5(3) |
| C7–N4 | 1.327(5) | O4–C7–N4 | 126.6(4) |

Conclusions

The goal of this study was to explore fundamental aspects of Fe(II)–CO–CN chemistry. This class of complexes is also potentially related to prebiotic processes and biosynthesis of the hydrogenase enzymes.⁴⁵

Stable Fe–CN–CO complexes form under very mild conditions by treatment of ferrous salts with CO and cyanide. Depending on the reaction conditions, either *trans*- $[\text{Fe}(\text{CN})_4(\text{CO})_2]^{2-}$ (**1**) or $[\text{Fe}(\text{CN})_5(\text{CO})]^{3-}$ (**3**) can be the dominant product. The *trans* dicarbonyl **1** converts to the pentacyanide **3** via a first-order (dissociative) pathway, as expected. The inefficient formation of *cis*- $[\text{Fe}(\text{CN})_4(\text{CO})_2]^{2-}$ (**2**) is curious in light of the apparent thermodynamic stability of this species. The nonobservation of $[\text{Fe}(\text{CN})_3(\text{CO})_3]^-$ ²⁰ and Fe(CN)₂(CO)₄ is attributed their high reactivity toward CN[−], leading to *trans*- $[\text{Fe}(\text{CN})_4(\text{CO})_2]^{2-}$ (**1**). We were able to prepare *fac*- $[\text{Ru}(\text{CN})_3(\text{CO})_3]^-$ with a preformed tricarbonyl complex, as well as confirm the structure of *fac*- $[\text{Mn}(\text{CN})_3(\text{CO})_3]^{2-}$.

Whereas the alkylation of cyanide ligands has been exhaustively examined,⁴⁶ the methylation of $[\text{Fe}(\text{CN})_5(\text{CO})]^{3-}$ (**3**) represents a rare study on the regiochemistry of methylation of a polycyano complex. The results support the view that CN *trans* to CN is more basic than CN *trans* to CO.

Experimental Section

General Considerations. Unless otherwise indicated, reactions were conducted using standard Schlenk techniques (N_2) at room temperature with stirring and solvents were dried via filtration through activated alumina. Elemental analyses were conducted by the University of Illinois Microanalytical Laboratory. ^1H NMR spectra were acquired on a Unity Varian 500 spectrometer. ^{13}C NMR (CD_3CN) measurements on PPh_4^+ salts gave signals at δ 118.90 (d), 131.35 (d), 135.69 (d), 136.41 (d), while for PPN^+ the aryl signals were observed at δ 128.20 (dd), 130.39 (m), 133.23 (m), 134.64 (s). ^1H NMR (CD_3CN) for PPN^+ : 7.65 (s), 7.55 (m), 7.45 (m). IR spectra were collected on a Mattson Infinity Gold FTIR spectrometer. ESI-MS were collected on a Quattro quadrupole–hexapole–quadrapole (QH) mass spectrometer. Cyclic voltammograms were measured at a scan rate of 200 mV/s on 10^{-3} M MeCN solutions using 0.01 M Bu_4NPF_6 as supporting electrolyte and referenced to $\text{Fc}^{+/0}$. A platinum wire counter electrode, a glassy carbon working electrode, and a $\text{Ag}|\text{AgPF}_6(\text{MeCN})$ reference electrode were used.

(45) Keefe, A. D.; Miller, S. L. *Origins Life Evol. Biosphere* **1996**, *26*, 111–129.

(46) Fehlhammer, W. P.; Fritz, M. *Chem. Rev.* **1993**, *93*, 1243–1280.

Reaction of FeCl₂ with Et₄NCN under CO. Under a CO atmosphere a solution of 0.127 g (1.00 mmol) of FeCl₂ in 10 mL of MeCN was treated with a solution of 0.624 g (4.00 mmol) of Et₄NCN in 10 mL of MeCN. After 8 h, the yellow solution was evaporated to dryness, and the residue was redissolved in 10 mL of H₂O. The aqueous extract was then slowly added to a solution of 0.75 g (2.0 mmol) of Ph₄PCl in 10 mL of H₂O. The white precipitate of *trans*-(PPh₄)₂[Fe(CN)₄(CO)₂] (**1**) and *cis*-(PPh₄)₂[Fe(CN)₄(CO)₂] (**2**) was filtered off and then extracted into 5 mL of MeCN. Addition of 50 mL of Et₂O to the MeCN extract induced precipitation of *trans*-(PPh₄)₂[Fe(CN)₄(CO)₂] (**1**). Yield: 0.345 g (39%). The aqueous filtrate from above was added to a solution of 1.15 g (2.0 mmol) of PPnCl in 300 mL of H₂O. The resulting white precipitate (PPN)₃[Fe(CN)₅(CO)] (**3**) was collected by filtration and washed with 10 mL of H₂O and 25 mL of Et₂O. Colorless powders of **3** became yellow upon drying. Yield: 0.66 g (36%).

***trans*-(PPh₄)₂[Fe(CN)₄(CO)₂] (**1**).** IR (CH₃CN): $\nu_{\text{CN}} = 2103$ (s); $\nu_{\text{CO}} = 1999$ (s) cm⁻¹. ¹³C NMR (126 MHz, CD₃CN): δ 212.84 (s, Fe–CO), 140.58 (s, Fe–CN). Anal. Calcd for C₅₄H₄₄FeN₄O₄P₂ (found): C, 69.68 (69.45); H, 4.76 (4.92); N, 6.02 (5.74).

(PPN)₃[Fe(CN)₅(CO)] (3**).** IR (CH₃CN): ν_{CN} 2090 (w), 2075 (s); ν_{CO} 1932 (s) cm⁻¹. IR (KBr): $\nu_{\text{CN}} = 2090$ (sh), 2075 (s); $\nu_{\text{CO}} = 1925$ (s) cm⁻¹. ESI-MS: $m/z = 1290.3$ ([PPN]₂[Fe(CO)(CN)₅]), 724.5 ([PPN][Fe(CO)(CN)₃]), 134.1 ([Fe(CN)₃]). ¹³C NMR (126 MHz, CD₃CN): 221.44 (s, Fe–CO), 157.77 (s, Fe–CN), 155.69 (s, Fe–CN). Anal. Calcd for C₁₁₄H₉₀FeN₈OP₆·0.5H₂O (found): C, 74.47 (73.96); H, 4.99 (4.67); N, 6.09 (6.39).

Reaction of FeCl₂ with Et₄NCN under CO in Refluxing MeCN. Under a CO atmosphere a solution of 0.127 g (1.00 mmol) of FeCl₂ in 10 mL of MeCN was treated with 0.624 g (4.00 mmol) of Et₄NCN in 10 mL of MeCN. After 8 h, the yellow solution was warmed to reflux for 18 h, producing a yellow suspension. The yellow solid (80 mg) (**4**) was collected by filtration. The colorless filtrate was evaporated to dryness, and the residue was extracted into 10 mL of H₂O. The aqueous extract was then slowly added to a solution of 0.38 g of Ph₄PCl in 10 mL of H₂O to give white *cis*-(PPh₄)₂[Fe(CN)₄(CO)₂] (**2**). Yield: 0.082 g (9%). The aqueous filtrate was added to a solution of 1.15 g (2.0 mmol) of PPnCl in 300 mL of H₂O to give a white precipitate, which was collected by filtration and washed with 10 mL of H₂O and 25 mL of ether. Yield: 0.98 g (54%). Note that (PPN)₃[Fe(CN)₅(CO)] (**3**) changes (reversibly) from colorless to yellow upon dehydration.

***cis*-(PPh₄)₂[Fe(CN)₄(CO)₂] (**2**).** IR (CH₃CN): $\nu_{\text{CN}} = 2119$ (w), 2108 (m); $\nu_{\text{CO}} = 2042$ (s), 1994 (s) cm⁻¹. ESI-MS: $m/z = 555.4$ ([PPh₄][Fe(CN)₄(CO)₂]), 499.4 ([PPh₄][Fe(CN)₄]), 134.1 ([Fe(CN)₃]). ¹³C NMR (126 MHz, CD₃CN): δ 211.85 (s, Fe–CO), 141.83 (s, Fe–CN), 139.68 (s, Fe–CN). Anal. Calcd for C₅₄H₄₀FeN₄O₂P₂ (found): C, 72.49 (72.60); H, 4.51 (4.35); N, 6.26 (6.60).

Yellow Solid (4**).** IR (KBr): 2995 (w), 2954 (w), 2215 (w), 2094 (s), 1995 (s), 1484 (m), 1456 (m), 1396 (m), 1307 (w), 1261 (w), 1184 (m), 1174 (m), 1035 (w), 1004 (m), 788 (m), 630 (m), 586 (m), 530 (w), 495 (m).

Reaction of **4 with Et₄NCN.** A solution of 0.05 g of Et₄NCN in 8 mL of MeCN was treated with 0.03 g of polymer **4**. After 30 min, the polymer was completely dissolved and checked by IR spectroscopy, which showed the formation of [Fe(CN)₅(CO)]³⁻.

Kinetics Study of the Reaction of *trans*-(PPh₄)₂[Fe(CN)₄(CO)₂] (1**) and CN⁻.** A solution of 0.07 g (0.078 mmol) of *trans*-(PPh₄)₂[Fe(CN)₄(CO)₂] (**1**) in 5 mL of MeCN (or EtCN) was treated with 0.122 g (0.78 mmol) of Et₄NCN at 51, 63, 82, and 96 °C. The buildup of product [Fe(CN)₅(CO)]³⁻ (**3**) was observed at 1932 cm⁻¹,

and the disappearance of the reactant *trans*-[Fe(CN)₄(CO)₂]²⁻ (**1**) was monitored at 1999 cm⁻¹. The reaction at 82 °C was complete in 120 min.

Preparative Scale Reaction of *trans*-(PPh₄)₂[Fe(CN)₄(CO)₂] (1**) and CN⁻.** A solution of 0.06 g (0.067 mmol) of *trans*-(PPh₄)₂[Fe(CN)₄(CO)₂] (**1**) and 0.025 g (0.068 mmol) of Ph₄PCN in 10 mL of MeCN was warmed to reflux for 6 h. During this time the reaction was monitored by IR spectroscopy. The IR spectrum showed the formation of (PPN)₃[Fe(CN)₅(CO)] (**3**). The solution was filtered to remove a small quantity of an insoluble impurity. The filtrate was evaporated to dryness, and the residue was redissolved in 5 mL of H₂O. The aqueous solution was slowly added to a solution of 0.75 g of PPnCl in 100 mL of H₂O to precipitate white **3**. Yield: 0.098 g (79%).

Thermolysis of *trans*-(PPh₄)₂[Fe(CN)₄(CO)₂] (1**).** A solution of 0.13 g of *trans*-(PPh₄)₂[Fe(CN)₄(CO)₂] (**1**) in 10 mL of MeCN was warmed to reflux for 12 h to give a yellow precipitate and a pale yellow solution. After removal of the yellow precipitate (0.01 g) by filtration, the colorless filtrate was evaporated to dryness. The residue was washed with 10 mL of H₂O to give a white suspension of *cis*-(PPh₄)₂[Fe(CN)₄(CO)₂] (**2**) (0.004 g), which was collected by filtration. The aqueous filtrate was added to a solution of 0.5 g of PPnCl in 100 mL of H₂O. The resulting white precipitate was collected by filtration and washed with 6 mL of H₂O and 25 mL of ether followed by drying in vacuo to produce a yellow solid of (PPN)₃[Fe(CN)₅(CO)] (**3**). Yield: 0.112 g (42%).

(PPN)₂[Fe(CN)₄(1,10-phenanthroline)]. A solution of 0.127 g (1.0 mmol) of FeCl₂ in 10 mL of MeCN was treated with 0.624 g (4.00 mmol) of Et₄NCN in 10 mL of MeCN, and a red solution formed. After 1 h of stirring, 0.18 g (1.0 mmol) of 1,10-phenanthroline in 5 mL of MeCN was added to the red solution and the solution turned blue. The blue solution was stirred overnight and then evaporated to dryness, and the residue was redissolved in 10 mL of H₂O to get a red aqueous solution. The aqueous solution was added to a solution of 1.5 g (2.6 mmol) of PPnCl in 300 mL of H₂O to give a blue precipitate, which was collected by filtration and washed with 10 mL of H₂O and 25 mL of ether followed by drying in vacuo to give blue (PPN)₂[Fe(CN)₄(C₁₂H₈N₂)]. Yield: 1.12 g (79%). IR (CH₃CN): $\nu_{\text{CN}} = 2062$ (s), 2079 (m), 2102 (w) cm⁻¹. ESI-MS: $m/z = 878.4$ ([PPN][Fe(CN)₄(C₁₂H₈N₂)]), 341 ([Fe(CN)₄(C₁₂H₈N₂)]), 134.1 ([Fe(CN)₃]). ¹H NMR (500 MHz, CD₃CN): δ 7.60 (dd), 7.88 (s), 8.17 (dd), 9.75 (br).

Methylation of (PPN)₃[Fe(CN)₅(CO)] (3**). Synthesis of *cis*-(PPN)₂[Fe(CN)₄(CNMe)(CO)].** A solution of 0.125 g (0.068 mmol) of (PPN)₃[Fe(CN)₅(CO)] (**3**) in 5 mL of MeCN was treated with 8 μ L (0.068 mmol) of MeOTf at -20 °C. After 0.5 h, the yellow solution was evaporated to dryness, and the residue was washed with 20 mL of H₂O. The solid was recrystallized from MeCN using Et₂O to give pale yellow microcrystals of *cis*-(PPN)₂[Fe(CN)₄(CNMe)(CO)] (**5**). Yield: 0.05 g (56%). IR (CH₃CN): $\nu_{\text{CN}} = 2189$ (m), 2111 (w), 2102 (m), 2090 (s); $\nu_{\text{CO}} = 1972$ (s) cm⁻¹. ESI-MS: $m/z = 767.3$ ([PPN][Fe(CN)₄(CNMe)(CO)]), 698.3 ([PPN][Fe(CN)₄]), 134.1 ([Fe(CN)₃]). ¹H NMR (500 MHz, CD₃CN): δ 3.30 (s, MeNC), ¹³C NMR (126 MHz, CD₃CN): δ 217.13 (s, Fe–CO), 149.93 (s, Fe–CN), 148.31 (s, Fe–CN), 147.86 (s, Fe–CN), 147.63 (s, Fe–CN). Anal. Calcd for C₇₉H₆₃FeN₇OP₂ MeCN (found): C, 71.97 (72.43); H, 4.82 (4.90); N, 7.71 (7.92).

Dimethylation of (PPN)₃[Fe(CN)₅(CO)] (3**).** A solution of 0.125 g of (PPN)₃[Fe(CN)₅(CO)] (**3**) in 5 mL of MeCN was treated with 16 μ L (0.137 mmol) of MeOTf at -20 °C. After 0.5 h, the yellow solution was evaporated to dryness, and the residue was washed with 20 mL of H₂O. The solid was recrystallized from MeCN using Et₂O to give white microcrystals of *fac*-(PPN)[Fe(CN)₅(CNMe)₂]

Table 8. Crystallographic Data for *trans*-(PPN)₂[Fe(CN)₄(CO)₂] (PPN-1), *cis*-(PPN)₂[Fe(CN)₄(CO)₂] (PPN-2), *cis*-(PPN)₂[Fe(CN)₄(CNMe)(CO)] (PPN-5), *fac*-(PPh₄)₂[Mn(CN)₃(CO)₃], and *fac*-(Na)[Ru(CN)₃(CO)₃]

| | | | | | |
|--|--|--|---|---|---|
| chem formula | C ₇₈ H ₆₀ FeN ₆ O ₂ P ₄ | C ₇₈ H ₆₀ FeN ₆ O ₂ P ₄ | C ₇₉ H ₆₃ FeN ₇ O ₄ | C ₁₁₁ H ₈₀ Cl ₉ Mn ₂ N ₆ O ₆ P ₄ | C ₉ H ₇ NaO ₄ Ru |
| temp (K) | 273(2) | 193(2) | 193(2) | 193(2) | 193(2) |
| cryst size (mm) | 0.64 × 0.20 × 0.014 | 0.48 × 0.32 × 0.25 | 0.24 × 0.22 × 0.20 | 0.04 × 0.08 × 0.11 | 0.16 × 0.08 × 0.08 |
| space group | <i>P</i> 2 ₁ / <i>n</i> | <i>Pbcn</i> | <i>P</i> 2 ₁ / <i>m</i> | <i>Pn</i> | <i>P</i> 2 ₁ / <i>n</i> |
| <i>a</i> (Å) | 12.955(3) | 23.840(6) | 10.853(13) | 16.008(2) | 10.488(5) |
| <i>b</i> (Å) | 13.213(3) | 20.405(5) | 25.38(3) | 16.968(2) | 10.395(5) |
| <i>c</i> (Å) | 20.003(5) | 19.321(5) | 15.45(2) | 19.521(3) | 12.870(6) |
| α (deg) | 90 | 90 | 90 | 90 | 90 |
| β (deg) | 106.528(4) | 90 | 110.42(2) | 99.147(3) | 106.679(8) |
| γ (deg) | 90 | 90 | 90 | 90 | 90 |
| <i>V</i> (Å ³) | 3282.7(13) | 9399(4) | 3988(9) | 5234.9(13) | 1344.1(11) |
| <i>Z</i> | 4 | 8 | 2 | 2 | 4 |
| <i>D</i> _{calcd} (Mg m ⁻³) | 1.308 | 1.306 | 1.088 | 1.362 | 1.740 |
| μ (Mo Kα, mm ⁻¹) | 0.381 | 0.320 | 0.313 | 0.589 | 1.211 |
| max./min. transm | 0.9929/0.8507 | 0.9952/0.9117 | 0.9976/0.8434 | 0.9222/0.9962 | 1.0000/0.80 |
| reflms measd/indep | 30337/8066 | 84518/11583 | 22259/5684 | 27471/14593 | 10696/3234 |
| data/restraints/params | 8066/0/412 | 11583/0/597 | 5684/0/431 | 14593/26/738 | 3234/0/172 |
| GOF | 1.007 | 1.100 | 0.918 | 0.735 | 0.993 |
| <i>R</i> _{int} | 0.0686 | 0.0569 | 0.0797 | 0.2495 | 0.0730 |
| <i>R</i> ₁ [<i>I</i> > 2σ] (all data) ^a | 0.046 (0.1087) | 0.0427 (0.0845) | 0.0502 (0.0916) | 0.0668 (0.3344) | 0.0382 (0.0603) |
| <i>R</i> _w [<i>I</i> > 2σ] (all data) ^{b,c} | 0.0958 (0.1109) | 0.1194 (0.1356) | 0.1097 (0.01203) | 0.0827 (0.1281) | 0.0874 (0.0964) |
| max. peak/hole (e ⁻ /Å ³) | 0.362/-0.319 | 0.349/-0.382 | 0.272/-0.274 | 0.490/-0.473 | 0.889/-0.655 |

$$^a R = \sum |F_o| - |F_c| / \sum |F_o|, \quad ^b R_w = \{[\sum (|F_o| - |F_c|)^2] / \sum [w F_o^2]\}^{1/2}, \quad ^c w = 1/\sigma^2(F_o).$$

(CO)] (**6**). Yield: 0.03 g (58%). IR (CH₃CN): ν_{CN} = 2223 (s), 2198 (s), 2113 (s), 2103 (w); ν_{CO} = 2009 (s) cm⁻¹. ESI-MS: *m/z* = 244.1 ([Fe(CN)₃(CNMe)₂(CO)]), 203.2 ([Fe(CN)₃(CNMe)(CO)]), 134.1 ([Fe(CN)₃]). ¹H NMR (500 MHz, CD₃CN): δ 3.37 (s, 6H, MeNC).

Protonation of (PPN)₃[Fe(CN)₅(CO)] (3**).** A solution of 0.62 g (0.339 mmol) of (PPN)₃[Fe(CN)₅(CO)] (**3**) in 10 mL of MeCN was treated with 30 μL (0.339 mmol) of HOTf at -20 °C. After 0.5 h, the colorless solution was evaporated to 3 mL, and 20 mL of Et₂O was added to give a white solid. The solid was recrystallized from MeCN using Et₂O to give white microcrystals of *cis*-(PPN)₂[Fe(CN)₄(CNH)(CO)]. Yield: 0.37 g (85%). IR (KBr): ν_{CN} = 2090 (s); ν_{CO} = 1973 (s) cm⁻¹. ESI-MS: *m/z* = 753.3 [(PPN)₂[Fe(CN)₄(CNH)(CO)]]. ¹H NMR (500 MHz, CD₃CN): δ 9.19 (s, 1H, HNC).

Reaction of FeCl₂ with Et₄NCN Followed by Carbonylation. A solution of 0.012 g (0.1 mmol) of FeCl₂ in 5 mL of MeCN was treated with 0.064 g (0.4 mmol) of Et₄NCN in 5 mL of MeCN, and a red solution formed immediately. After 1 h, the red solution was purged with CO for 5 h to give an orange solution. The reaction was monitored by FT-IR spectroscopy, which showed the predominant formation of [Fe(CN)₅(CO)]³⁻ (**3**) and a minor quantity of *trans*-[Fe(CN)₄(CO)₂]²⁻ (**1**).

Aqueous Reaction of FeCl₂ with KCN under CO. Under an atmosphere of CO, an aqueous solution of 0.127 g (1.00 mmol) of FeCl₂ in 10 mL of H₂O was treated with 0.26 g (4.00 mmol) of KCN in 5 mL of H₂O. After 5 h, the resulting yellow solution was slowly added to a solution of 0.75 g of PPh₄Cl in 10 mL of H₂O to yield 0.08 g (9%) of white *trans*-(PPh₄)₂[Fe(CN)₄(CO)₂] (**1**) together with trace amounts of *cis*-(PPh₄)₂[Fe(CN)₄(CO)₂] (**2**, detected by IR spectroscopy). The aqueous solution was treated with a solution of 1.5 g of PPNCl in 300 mL of H₂O to precipitate pale yellow (PPN)₃[Fe(CN)₅(CO)] (**3**). Yield: 0.6 g (32%).

Oxidation of (PPN)₃[Fe(CN)₅(CO)] (3**).** A solution of 0.250 g (0.136 mmol) of (PPN)₃[Fe(CN)₅(CO)] (**3**) in 10 mL of MeCN was treated with 0.045 g (0.068 mmol) of FcPF₆ in 5 mL of MeCN. The yellow solution turned to red-brown immediately. After 1 h, the solvent was evaporated to dryness, and the remaining red-brown oil was washed with 10 mL of Et₂O. The product was purified by precipitation from 5 mL of MeCN using 20 mL of Et₂O to give a

red solid of (PPN)₂[Fe(CN)₅(CO)] (**7**). Yield: 0.105 g (59%). IR (CH₃CN): ν_{CN} = 2127 (w), 2096 (s); ν_{CO} = 1980 (s) cm⁻¹.

***fac*-(PPh₄)₂[Mn(CN)₃(CO)₃].** A 50-mL Teflon lined stainless steel bomb was charged with 0.35 g (1.52 mmol) of Mn(CO)₅Cl, 0.3 g (4.61 mmol) of KCN, and 20 mL of EtOH. The reaction mixture was then heated to 120 °C for 72 h. After cooling, the bomb was opened in air, and the reaction mixture was extracted with 100 mL of warm (50 °C) EtOH. The colorless extract was evaporated to dryness. The residue was extracted into ~5 mL of H₂O, and this extract was added dropwise to a solution of 1.5 g (4.00 mmol) of PPh₄Cl in 30 mL of H₂O. The resulting white precipitate was collected by filtration and purified by precipitation from 5 mL of MeCN using 40 mL of Et₂O. The resulting solid was washed with 20 mL of Et₂O. Yield: 0.75 g (55%). IR (CH₃CN): ν_{CN} = 2110 (w), 2097 (m); ν_{CO} = 1993 (s), 1904 (s) cm⁻¹. Anal. Calcd for C₅₄H₄₂MnN₃O₄P₂ (found): C, 70.98 (70.70); H, 4.63 (4.55); N, 4.60 (4.30).

***fac*-(PPh₄)₂[Ru(CN)₃(CO)₃].** A solution of 0.5 g (1.91 mmol) of RuCl₃ in 20 mL of 2-ethoxyethanol was purged with a stream of CO while warming to reflux as described previously.⁴⁷ The initial brown-black color turned yellow over the course of 3 h. The solution was allowed to cool to 25 °C under CO and maintained under CO for 7 h. The solvent was evaporated to dryness, and the residue was extracted into 20 mL of MeOH. This extract was treated with 0.28 g (5.73 mmol) of NaCN under CO. After 18 h, the colorless solution was evaporated to dryness, and the residue was extracted into 10 mL of H₂O. The aqueous solution was then slowly added to a solution of 0.75 g of PPh₄Cl in 10 mL of H₂O. The resulting white precipitate was recrystallized from MeCN by the addition of Et₂O. Yield: 350 mg (55%). IR (CH₃CN): ν_{CN} = 2163 (m), 2144 (w); ν_{CO} = 2117 (s), 2075 (s) cm⁻¹. ESI-MS: *m/z* = 264.0 ([Ru(CO)₃(CN)₃]), 236.0 ([Ru(CN)₃(CO)₂]), 208.0 ([Ru(CN)₃(CO)]), 180.1 ([Ru(CN)₃]). ¹³C NMR (126 MHz, CD₃CN): δ 122.99 (s, Ru-CN), 187.62 (s, Ru-CO). Anal. Calcd for C₃₀H₂₀N₃O₃PRu (found): C, 59.80 (59.49); H, 3.35 (3.25); N, 6.97 (6.90).

Crystallography. Crystals of *trans*-(PPN)₂[Fe(CN)₄(CO)₂] (PPN-1), *cis*-(PPN)₂[Fe(CN)₄(CO)₂] (PPN-2), *cis*-(PPN)₂[Fe(CN)₄(CNMe)(CO)] (PPN-5), *fac*-(PPh₄)₂[Mn(CN)₃(CO)₃], and *fac*-Na(DMF)-

(47) Luga, N.; Lavigne, G.; Soulie, J. M.; Fabre, S.; Kalck, P.; Saillard, J.-Y.; Halet, J. F. *Organometallics* **1995**, *14*, 1712–1731.

[Ru(CN)₃(CO)₃] were mounted on a thin glass fiber by using oil (Paratone-N, Exxon) before being transferred to the diffractometer. Data were collected on a Siemens CCD automated diffractometer at low temperature. Data processing was performed with the integrated program package SHELXTL.⁴⁸ All structures were solved using direct methods and refined using full-matrix least squares on F^2 using the program SHELXL-97.⁴⁹ All hydrogen atoms were fixed in idealized positions with thermal parameters 1.5 times those of the attached carbon atoms. The data were corrected for absorption on the basis of Ψ scans. Specific details for each crystal are given in Table 8. Full crystallographic data for each compound have been deposited with the Cambridge Crystallographic Data Center as

(48) Sheldrick, G. M. *SHELXTL*; Bruker AXS: Madison, 1998.

(49) Sheldrick, G. M. *SHELXL-97*; University of Göttingen: Göttingen, 1997.

supplementary publication no. CCDC-170080 (PPN-1), 170081 (PPN-2), 170083 (PPN-5), 163659 (*fac*-(PPh₄)₂[Mn(CN)₃(CO)₃]), and 171511 (*fac*-Na(DMF)[Ru(CN)₃(CO)₃]).

Acknowledgment. This research was supported by U.S. Department of Energy and National Institutes of Health.

Supporting Information Available: Eyring plot for cyanation of *trans*-[Fe(CN)₄(CO)₂]²⁻ (**1**), molecular structure of the anion *fac*-Na(DMF)[Ru(CN)₃(CO)₃]⁻ with thermal ellipsoids drawn at the 50% level, and X-ray crystallographic files in CIF format and listings of positional and thermal parameters which do not appear in the text. This material is available free of charge via the Internet at <http://pubs.acs.org>.

IC011030L